

# Watt-level output rectangular-core neodymium-doped silicate glass fiber laser

Wentao Li (李文涛)<sup>1,2</sup>, Danping Chen (陈丹平)<sup>1,\*</sup>, Qinling Zhou (周秦岭)<sup>1</sup>,  
and Lili Hu (胡丽丽)<sup>1</sup>

<sup>1</sup>Shanghai Institute of Optics and Fine Mechanics, Chinese Academy of Sciences, Shanghai 201800, China

<sup>2</sup>University of Chinese Academy of Sciences, Beijing, China

\*Corresponding author: dpchen2008@aliyun.com

Received August 19, 2015; accepted November 6, 2015; posted online December 17, 2015

We produce a maximum 1.45 W laser output at 1064 nm using a neodymium-doped silicate glass fiber that has a rectangular core with dimensions of  $\sim 6.3 \mu\text{m} \times 31.5 \mu\text{m}$ . The measured divergence angles of the output laser in two dimensions are  $3.22^\circ$  and  $1.76^\circ$ , respectively. The output power is stable and limited only by the available pump power.

OCIS codes: 060.2280, 060.3510, 140.3530, 160.2290.

doi: 10.3788/COL201614.011402.

A rectangular-core fiber, also known as a ribbon fiber, has attracted much attention for fiber lasers and amplifiers due to its good thermal capacity. Conventional circular-core optical fibers face power scaling limitations from thermal lensing and stimulated Raman scattering<sup>[1]</sup>, while a ribbon fiber can operate in a high-order mode (HOM) that can overcome the obstacles by increasing the mode area without becoming thermal lens limited and without the on-axis intensity peak associated with circular HOMs<sup>[2]</sup>. In 2008, Dawson *et al.* suggested that the power scaling in a single-core circular fiber (silica glass fiber) is limited to roughly 40 kW<sup>[3]</sup>. Compared to traditional circular core fibers, the rectangular-core fibers have many more advantages and applications including more efficient heat removal because the long dimension of a rectangular core increases the surface area for heat removal<sup>[4]</sup>, large mode area, high birefringence, easily pumped by semiconductor lasers because their initial output laser beam shapes were rectangular, and used as rectangular-core waveguides<sup>[5]</sup>. Because propagation of a higher-order mode in a ribbon fiber allows for better thermal management and bend-loss immunity than conventional circular-core fibers, rectangular-core fibers were also used in laser amplification by mode-converters in recent years<sup>[6-8]</sup>. High-order ribbon fiber modes can be converted to a fundamental Gaussian mode with a high efficiency for applications. In 2012, Sridharan *et al.* presented the first simulation and experimentation of the mode conversion technique and demonstrated a mode-converter system that converts a single HOM of a ribbon fiber back to a diffraction-limited TEM<sub>00</sub> mode with the conversion efficiency 80.5%<sup>[9]</sup>. In 2015, Drachenberg *et al.* design process resulted in a 1.7 m  $500 \times 34 \mu\text{m}$  core-ribbon fiber amplifier that could theoretically achieve 10 kW of output power in a single frequency and a single HOM<sup>[6]</sup>. This mode conversion technique makes the rectangular-core fibers have greater potential applications in laser amplifiers than the traditional circular-core large mode area fibers<sup>[2,10,11]</sup>.

Up to now, the ribbon fiber was usually based on pure silica glass. However, as important materials for fiber manufacture, multicomponent glass, including silicate glass, phosphate glass, tellurite glass, and chalcogenide glass show the following unique advantages over pure silica glass: a wider adjustable range of refractive index, and lower melting and processing temperatures (usually below  $1000^\circ\text{C}$ )<sup>[12]</sup>. In addition, the rare earth solubility is higher than that of silica, enabling higher and more homogeneous rare-earth doping concentration<sup>[13-16]</sup>. Thus, a relatively short fiber length can be used for laser generation that compensates the higher loss caused by the multicomponent glass compared to silica glass.

In this Letter, we have reported on a rectangular-core neodymium-doped (Nd-doped) silicate glass fiber that has a rectangular-shape laser output; the maximum output power was 1.45 W with 1 m length fiber. The fiber has different divergence angles in the long dimension and short dimension of the fiber core.

The fiber studied is made from two kinds of silicate glasses ( $\text{SiO}_2\text{-B}_2\text{O}_3\text{-BaO-Na}_2\text{O-K}_2\text{O}$ ) made by the melting method, namely G1 and G2. The G2 glass was doped with rare earth ion  $\text{Nd}^{3+}$ . The active dopant level is 1.2 wt.%, which was employed as an active core element. The two kinds of glasses are thermally stable and have compatible properties. Moreover, their thermal expansion and softening temperatures are similar. The measured rod-drawing temperatures of these two glasses are  $810^\circ\text{C}\text{--}840^\circ\text{C}$  and  $830^\circ\text{C}\text{--}860^\circ\text{C}$ , respectively. The refractive indices of the G1 and G2 glasses were measured using a prism coupling technique at 5 distinct wavelengths given as follows: 486.1, 587.6, 632.8, 1053, and 1552 nm. The accuracy of the refractive indices measurement was  $5 \times 10^{-5}$ . The measured results were fitted using Sellmeier's equation. The obtained refractive indices by Sellmeier's equation of the two kinds of glasses G1 and G2 were 1.5067 and 1.5122 at 1064 nm, respectively. The other main relevant detailed physical parameters of G1 and G2 are provided in Table 1.

**Table 1.** Detailed Physical Parameters of G1 and G2 Glasses

Glass	$T_g$ ( $^{\circ}\text{C}$ )	$T_{10}^{7.6}$ ( $^{\circ}\text{C}$ )	$\alpha_{100/300}$ ( $10^{-7}/\text{K}$ )	$\rho$ ( $\text{g}/\text{cm}^3$ )
G1	560	734	96	2.52
G2	580	746	88	2.51

In the table,  $T_g$  is the glass transformation temperature,  $T_{10}^{7.6}$  is the softening point,  $\alpha_{100/300}$  is the coefficient of thermal expansion at a temperature range from  $100^{\circ}\text{C}$  to  $300^{\circ}\text{C}$ , and  $\rho$  is the density of the glass at a temperature of  $20^{\circ}\text{C}$ . Those parameters show that the two kinds of silicate glasses were very suitable for the fabrication of the fiber.

The fiber was fabricated using the stack and draw technique. First, the Nd-doped glass G2 was processed into a rectangular cross section rod of the size  $1\text{ mm} \times 5\text{ mm} \times 80\text{ mm}$ . The G1 glass was processed into a  $22\text{ mm}$  diameter rod, which was drawn into  $1\text{ mm}$  diameter thin rods using a fiber-drawing tower in the following step. Second, the thin rods were arranged in an inner hexagonal mold, the innermost five rods in the X scale (long dimension) were replaced by the rectangular rod made by G2 to obtain a preform which is in accordance with the structure from the fiber design. Lastly, the preform was drawn into a fiber. A cross section of the end face of the rectangular core fiber produced in the experiment is shown in Fig. 1.

Due to the softening temperature of the G2 glass being slightly higher than that of the G1 glass, the fiber core maintains a rectangular shape perfectly by controlling a suitable fiber-drawing temperature. Considering the stress at the glass surface, the final cross section of the fiber is circular.

The fiber core size was measured at  $6.3\text{ }\mu\text{m} \times 31.5\text{ }\mu\text{m}$ , with an NA of 0.129 and an outer diameter of  $110\text{ }\mu\text{m}$ . The fiber has a pumping power absorption coefficient of about  $10\text{ dB}/\text{m}$  at  $793\text{ nm}$  and  $4\text{ dB}/\text{m}$  loss at  $1550\text{ nm}$  using the standard cutback method. A plane-parallel Fabry-Perot resonator was constructed to measure the laser efficiency of the fiber pumped by a diode laser at a wavelength of

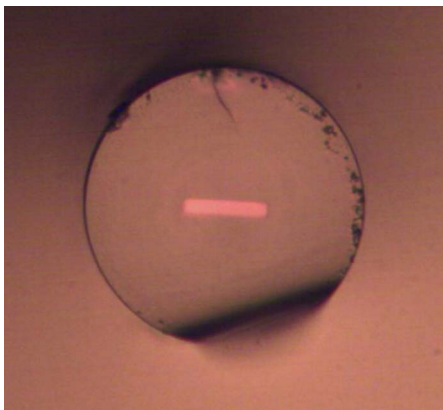
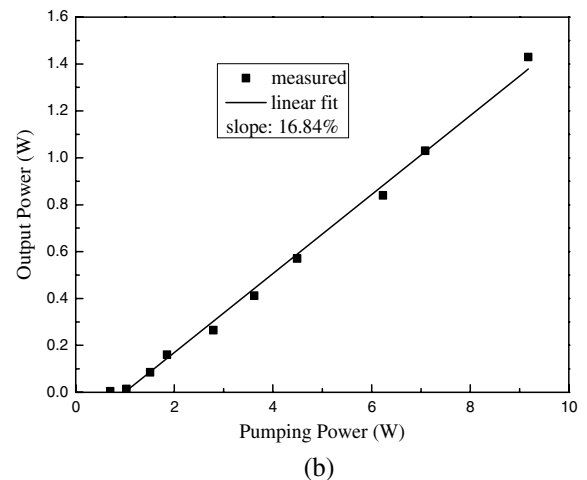
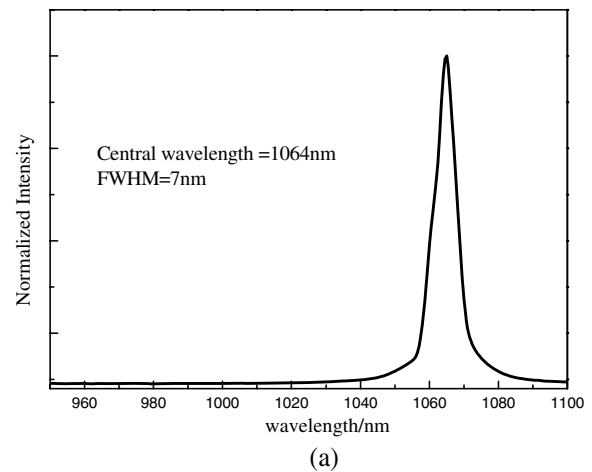


Fig. 1. Cross section of the end face of the fiber.

$793\text{ nm}$ . The pumped laser beam from a coupled transmission fiber was collimated by an aspherical lens with an NA of 0.25 with an  $11\text{ mm}$  focal length. After that, the beam was focused into the fiber by another aspherical lens with an NA of 0.3 and a focal length of  $6.16\text{ mm}$ . A dichroic mirror (transmission of 99% at  $793\text{ nm}$ , reflectivity of 99% at  $1064\text{ nm}$ ) was butt-coupled to the fiber. The fiber output end face with about 5% Fresnel reflection raised by fiber cutting worked as another cavity mirror. A filter with a long-wave pass filter lens (transmission is less than 0.5% when the light wavelength is shorter than  $980\text{ nm}$ ) was inserted before the optical spectrometer or power meter to make sure that the pump light was eliminated and only the emission light was detected.

The fiber output laser spectrum was measured by a fiber spectrum analyzer (Blue-Wave Miniature Spectrometers, StellarNet, Inc.). One meter length fiber was used in the laser experiment. A maximal output power of  $1.45\text{ W}$  for  $9.18\text{ W}$  pumping power was generated; the maximal output powers were stable and limited only by the available pump power. Figure 2(a) shows the output characteristics and the spectrum of the fiber laser at the output power of

Fig. 2. (a) Measured spectrum of the fiber laser at an output power of  $1.45\text{ W}$ ; (b) measured output power as a function of the pumping power.

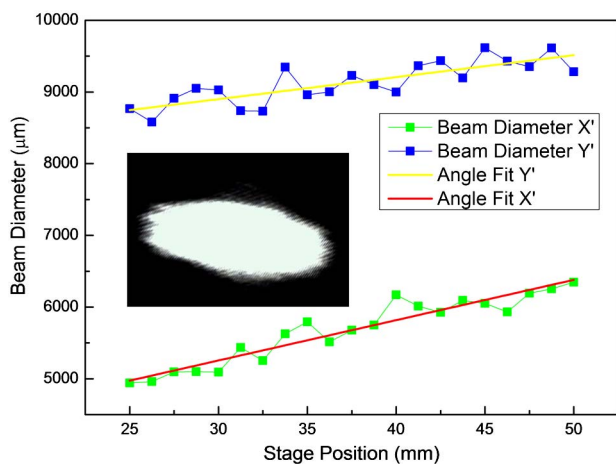


Fig. 3. Measured divergence angles in two orthogonal directions  $X$  and  $Y$ ; inset is the near-field intensity distribution of the output laser which was measured by the CCD.

1.45 W. The central wavelength of the output laser was 1064 nm and the measured full width at half maximum (FWHM) linewidth is 7 nm. Figure 2(b) shows that the measured slope efficiency with respect to pumping power was 16.84%. In addition, the near-field image of the laser beam across the fiber facet was recorded by a CCD at the output power of 1.45 W and the divergence angles in two orthogonal directions  $X$  and  $Y$  were measured by a beam profiler (Thorlabs BP109-IR2), as shown in Fig. 3. The near-field image of the laser beam was inserted in Fig. 3 as an inset, the horizontal direction was  $X$ , and the vertical direction was  $Y$ . The divergence angle in the  $X$  and  $Y$  directions was  $3.22^\circ$  and  $1.76^\circ$ , respectively. It has different divergence angles in each of the two directions and the divergence angle in the  $Y$  direction was almost half that of the  $X$  direction. The fiber has a potential to realize the single-mode output in the  $Y$  direction by designing the fiber structure and choosing the proper refractive index glass. This single-direction single-mode rectangular-shape laser is useful for many applications such as cutting and alignment marking.

In conclusion, we successfully design and fabricate Nd-doped silicate glass rectangular-core fiber and experimentally demonstrate a maximal output power of 1.45 W continuous-wave laser output and a slope efficiency of

16.84% is achieved at 1064 nm from a 1 m length fiber. The fiber has different divergence angles in the two directions. The divergence angles in the  $X$  and  $Y$  directions are  $3.22^\circ$  and  $1.76^\circ$ , respectively. The difference gives the fiber a potential to realize the single-mode output in a single direction. The relevant work has been started.

This work was supported by the Chinese National Natural Science Foundation under Grant No. 51272262.

## References

1. D. J. Richardson, J. Nilsson, and W. A. Clarkson, *J. Opt. Soc. Am. B* **27**, B63 (2010).
2. S. Yerolatsitis and T. A. Birks, *J. Lightwave Technol.* **33**, 1182 (2015).
3. J. W. Dawson, M. J. Messerly, R. J. Beach, M. Y. Shverdin, E. A. Stappaerts, A. K. Sridharan, P. H. Pax, J. E. Heebner, C. W. Siders, and C. P. J. Barty, *Opt. Express* **16**, 13240 (2008).
4. J. Dawson, A. Bullington, J. Heebner, M. Messerly, P. Pax, A. Sridharan, B. Ward, and C. Carlson, *Ribbon Fiber Geometry for Power Scaling in Continuous Wave Fiber Lasers* (Lawrence Livermore National Laboratory (LLNL), 2011).
5. F. Ladouceur, J. D. Love, and I. M. Skinner, *IEE Proc. J. Optoelectron.* **138**, 253 (1991).
6. D. Drachenberg, M. Messerly, P. Pax, A. Sridharan, J. Tassano, and J. Dawson, *Proc. SPIE* **8601**, 860107 (2013).
7. D. R. Drachenberg, M. J. Messerly, P. H. Pax, A. K. Sridharan, J. B. Tassano, and J. W. Dawson, *Proc. SPIE* **8961**, 89610T (2014).
8. W. L. Yang, T. Geng, J. Yang, J. Q. Diao, Y. Z. Wang, and H. T. Chen, *Sens. Lett.* **10**, 1397 (2012).
9. A. K. Sridharan, P. H. Pax, J. E. Heebner, D. R. Drachenberg, J. P. Armstrong, and J. W. Dawson, *Opt. Express* **20**, 28792 (2012).
10. A. L. Bullington, P. H. Pax, A. K. Sridharan, J. E. Heebner, M. J. Messerly, and J. W. Dawson, *Appl. Opt.* **51**, 84 (2012).
11. R. M. Tao, L. Huang, P. Zhou, L. Si, and Z. J. Liu, *Photonics Res.* **3**, 192 (2015).
12. X. Jiang, T. G. Euser, A. Abdolvand, F. Babic, F. Tani, N. Y. Joly, J. C. Travers, and P. S. Russell, *Opt. Express* **19**, 15438 (2011).
13. L. Hu, S. Chen, J. Tang, B. Wang, T. Meng, W. Chen, L. Wen, J. Hu, S. Li, and Y. Xu, *High Power Laser Sci. Eng.* **2**, e1 (2014).
14. C. Ma, J. Qiu, D. Zhou, Z. Yang, and Z. Song, *Chin. Opt. Lett.* **12**, 081601 (2014).
15. J. Boguslawski, J. Sotor, G. Sobon, R. Kozinski, K. Librant, M. Aksienionek, L. Lipinska, and K. M. Abramski, *Photonics Res.* **3**, 119 (2015).
16. Y. Miao, H. Zhang, H. Xiao, and P. Zhou, *Chin. Opt. Lett.* **12**, 091403 (2014).